IIE Transactions (2014) **46**, 1079–1092

ISSN: 0740-817X print / 1545-8830 online
DOI: 10.1080/0740817X.2014.882039

Drop fragility of the display of a smart mobile phone: weakest link failure or cumulative shock failure?

MINSU KIM[1] and SUK JOO BAE[2,*]

[1]*Development Team, Samsung Display Co., Cheonan, Republic of Korea*
[2]*Department of Industrial Engineering, Hanyang University, Seoul, 133-791, Republic of Korea*
E-mail: sjbae@hanyang.ac.kr

Received March 2013 and accepted October 2013

It is not unusual for portable devices to be damaged when they are accidentally dropped on hard floors. Shock tests are increasingly being used to evaluate the drop impact response of portable devices. However, the underlying failure mechanisms have not been fully theoretically explored. There are two candidate failure mechanisms that can account for the drop impact fragility of the display in a smart mobile phone during a shock test: weakest link failure and cumulative damage failure. The weakest link theory provides a basis on a Weibull distribution and the cumulative damage theory on an inverse Gaussian distribution. This article proposes a discrimination procedure for the two distribution types. The probability of correct selection is computed using asymptotic results on the ratio of the Maximum Likelihood (ML) to discriminate between the two distributions. Expressions are provided that can be used to compute the asymptotic distributions of ML estimators or their functions when there is model mis-specification. The proposed method is applied to real shock test data for smart mobile phone display modules to determine the underlying failure mechanisms.

Keywords: Discrimination, inverse Gaussian distribution, model mis-specification, probability of correct selection, shock damage, smart mobile phone, Weibull distribution

1. Introduction

Rapid developments in the telecommunications industry in the last decade have facilitated the widespread use of portable electronic devices such as digital cameras, mobile phones, and tablet Personal Computers (PCs). However, portable devices are often accidentally dropped onto hard floors due to inadvertent handling while using a device. This may cause the plastic housing of the device to fracture, assemblies to come apart, and fragile components such as the liquid crystal display and organic light-emitting diode to crack. Drop-induced failure is a dominant failure mode of portable electronic products. The forces and accelerations experienced by the portable electronic device during impact with a hard surface depend on the drop height, mass, impact orientation, and the surface on which the device is dropped (Lim *et al.*, 2002). Most existing studies on impact-proof designs have been confined to packaging or cushioning design (Goyal *et al.*, 1997). With the advent of expensive portable electronic devices such as Smart Mobile Phones (SMPs) and tablet PCs, the device's capability to survive the damage created by an accidental drop has become an important design requirement. Evaluation of the physical strength of a product must be preceded by the creation of products that can accommodate occasional severe impacts or sustain minimal damage from drop impacts. Durability and fragility have traditionally been evaluated using physical drop tests on prototypes. Although experimental drop tests allow direct and accurate evaluation on product is robustness, these tests are expensive and time-consuming to performs. Moreover, if the ability to survice a severe drop shock is unsatisfactory, the prototypes may have to be redesigned through a painful correction process.

The research presented in this article is motivated by one of the current critical issues associated with SMPs: display damage resulting from an accidental drop during usage. Because of customer demand for versatile functions and attractive SMP designs, the displays of SMPs have increased in size and this part of the device is more vulnerable than the other components to accidental shocks. SMP manufacturers perform drop tests to evaluate the device is fragility caused by a drop shock, focusing mainly on the display's structure. The drop test increases the drop height of the device until failure is observed; however, impact angle or impact area cannot be accurately controlled in drop tests.

*Corresponding author
Color versions of one or more of the figures in the article can be found online at www.tandfonline.com/uiie.

A (impact) shock test, which assesses drop impact on a targeted area, has been proposed and is increasingly being used. In a shock test, we support the device with a fixture on the carriage of a shock test machine and the carriage is dropped to deliver a given level of shock to the device at a fixed height. The impact angle and area can be adjusted in this test and the test machines can also control impact acceleration (as a degree of shock measure) and shock pulse to be loaded. This shock test involves gradually increasing the impact acceleration and continues until failure is observed. In general, durability to drop shock is evaluated by a Damage Boundary Curve (DBC). The DBC was first suggested by Newton (1968) to quantify the fragility of mechanical/electronic products in response to a drop impact. The formal procedure to draw a DBC is specified in ASTM D3332-99 (ASTM, 1999). The DBC is based on the weakest link theory, which states that an item's strength is limited to the weakest link or part that cannot sustain a threshold stress, even if the smallest impact is loaded. However, the exact physical mechanisms that lead to cracking of SMP displays in response to a drop shock have not yet been satisfactorily identified.

In this article, we propose a discrimination procedure to select the best model for drop impact durability of SMP displays in a shock test. This procedure is based on two candidate failure mechanisms: weakest link failure and cumulative shock failure. The weakest link theory is based on a Weibull distribution, which has been widely used in the fields of reliability and biostatistics. The cumulative damage theory is based on an inverse Gaussian distribution that is derived as the time to first passage of a Wiener process with a positive drift to a fixed threshold level. The inverse Gaussian distribution has been previously applied to the tensile strength of carbon fibers and fibrous carbon composite materials (Durham and Padgett, 1997).

The problem of testing whether some given data follows one of two candidate distributions has been extensively studied in the literature on statistics. The idea of discriminating between two distributions was originally proposed by Cox (1961). Chambers and Cox (1967) and Atkinson (1970) provided significant theoretical contributions to this discrimination problem. In particular, special attention has been paid to discriminating between lognormal and Weibull distributions (Dumonceaux and Antle, 1973; Pereira, 1978; Chen, 1980; Quesenberry and Kent, 1982; Kundu and Manglick, 2004; Pascual, 2005), gamma and Weibull distributions (Bain and Englehardt, 1980; Fearn and Nebenzahl, 1991), gamma and lognormal distributions (Kundu and Manglick, 2005), lognormal and generalized exponential distributions (Kundu *et al.* 2005), Weibull and generalized exponential distributions (Gupta and Kundu, 1951), and normal and extreme value distributions for a linear regression model (Yu, 2007). Recently, Tsai *et al.* (2011) investigated the mis-specification effect on the prediction of a product's Mean-Time-to-Failure (MTTF) when a Wiener process or gamma process was wrongly fitted to the degradation data. To the best of our knowledge, however, no studies have reported how to discriminate between Weibull and inverse Gaussian distributions.

In this article, we provide expressions to compute the asymptotic distribution of Maximum Likelihood Estimators (MLEs) under the Weibull and inverse Gaussian distributions when there is model mis-specification. We use the analytical approach proposed in White (1982a) to address the effects of model mis-specification on the properties of interest; e.g., distribution quantiles and MTTF. To discriminate between Weibull and inverse Gaussian distributions, we also compute the Probability of Correct Selection (PCS) using asymptotic results for the Ratio of the Maximum Likelihood (RML).

The rest of this article is organized as follows. In Section 2, we derive the quasi-MLEs of the Weibull and inverse Gaussian distributions under model mis-specification. Then, we compute the accuracy and precision of failure-time characteristics based on the quasi-MLEs when a distribution is wrongly fitted. In Section 3, we illustrate the computation of the PCS between the Weibull and inverse Gaussian distributions, based on the asymptotic distribution of the RML. Real shock test data for SMP display modules are analyzed in Section 4. Some numerical experiments are performed in Section 5. We conclude in Section 6 with a discussion on future research and concluding remarks.

2. Mis-specification between Weibull and inverse Gaussian distributions

2.1. *MLEs under no model mis-specification*

Suppose that there is a single item with length or size l that is divided into several independent sections. The item's strength, $S(l)$, is viewed as the minimum strength of the independent sections as an expression of the weakest-link size effect. This theory suggests that the distribution function of strength for an item with length l, $F(x;l) = \Pr[S(l) \le x]$, should satisfy the relation

$$\begin{aligned}\Pr[S(l) > x] &= 1 - F(x;l) = \{1 - F(x;1)\}^l \\ &= \{\Pr(S(1) > x]\}^l . \end{aligned} \tag{1}$$

A Weibull distribution, denoted by model M_1, is the only type of distribution that satisfies Equation (1), and the probability density function (p.d.f.) of the Weibull distribution with scale parameter $\lambda(>0)$ and shape parameter $\beta(>0)$ is

$$M_1 : f_{\mathrm{WE}}(x;\lambda,\beta) = \beta\lambda^\beta x^{\beta-1}\exp\left\{-(\lambda x)^\beta\right\}. \tag{2}$$

The mean and variance of the Weibull distribution are $\lambda^{-1}\Gamma(1+1/\beta) = (\lambda\beta)^{-1}\Gamma(1/\beta)$ and $\lambda^{-2}[\Gamma(1+2/\beta) - \Gamma(1+1/\beta)^2]$, respectively, where $\Gamma(\cdot)$ is the gamma function. The Weibull pth quantile is $x_p = \lambda^{-1}[-\ln(1-p)]^{1/\beta}$.

Based on cumulative damage theory, an inverse Gaussian distribution, denoted by model M_2, was introduced to model the strength of an item with length or size l (see Durham and Padgett (1997) and Onar and Padgett (2000)). The p.d.f. of the inverse Gaussian is

$$M_2 : f_{\mathrm{IG}}(x;\mu,\kappa) = \sqrt{\frac{\kappa}{2\pi x^3}} \exp\left\{-\frac{\kappa(x-\mu)^2}{2\mu^2 x}\right\}, \quad (3)$$

where the parameter $\mu(>0)$ is the mean of the distribution and $\kappa(>0)$ is a scale parameter. The variance of the inverse Gaussian distribution is μ^3/κ, implying that μ is not a location parameter in the usual sense. The shape parameter of the distribution is defined by $\phi = \kappa/\mu$, which is invariant under changes of scale. The cumulative distribution function (c.d.f.) of the inverse Gaussian is

$$F_{\mathrm{IG}}(x;\mu,\kappa) = \Phi\left[\sqrt{\frac{\kappa}{x}}\left(\frac{x}{\mu}-1\right)\right] + \exp\left\{\frac{2\kappa}{\mu}\right\} \times \Phi\left[-\sqrt{\frac{\kappa}{x}}\left(\frac{x}{\mu}+1\right)\right],$$

where $\Phi(\cdot)$ is the standard normal c.d.f. There is no simple closed-form expression for the inverse Gaussian pth quantile, thus it must be computed by numerically inverting $p = F_{\mathrm{IG}}(x_p;\mu,\kappa)$.

To derive MLEs for the two distributions, suppose $x_1,\ldots,x_n$ are random samples from either one of the two distribution functions. Based on the samples $x_1,\ldots,x_n$, the log-likelihood function of the Weibull distribution is defined by

$$\begin{aligned}\mathcal{L}_{\mathrm{WE}}(\lambda,\beta) &= \sum_{i=1}^{n} \ln f_{\mathrm{WE}}(x_i;\lambda,\beta) \\ &= n\ln\beta + n\beta\ln\lambda + \sum_{i=1}^{n}\left\{(\beta-1)\ln x_i - (\lambda x_i)^{\beta}\right\},\end{aligned} \quad (4)$$

and the MLEs of $\theta_1 \equiv (\lambda,\beta)$ for the Weibull distribution, $\hat{\theta}_1 \equiv (\hat{\lambda},\hat{\beta})$, satisfy the following relationship:

$$\hat{\lambda} = \left(n/\sum_{i=1}^{n} x_i^{\hat{\beta}}\right)^{1/\hat{\beta}}.$$

By denoting $\xrightarrow{\text{a.s.}}$ as the almost sure convergence, the MLEs $\hat{\theta}_1 \xrightarrow{\text{a.s.}} \theta_{1,0} \equiv (\lambda_0,\beta_0)$ as $n\to\infty$ under no model mis-specification, where (λ_0,β_0) are the values satisfying the following condition:

$$E_{M_1}(\mathcal{L}_{\mathrm{WE}}(\lambda_0,\beta_0)) = \max_{\tilde{\lambda},\tilde{\beta}} E_{M_1}\left(\mathcal{L}_{\mathrm{WE}}(\tilde{\lambda},\tilde{\beta})\right), \quad (5)$$

and $\sqrt{n}(\hat{\theta}_1 - \theta_{1,0})$ is asymptotically normal with mean of $\mathbf{0}$ and the variance–covariance matrix $\hat{\Sigma}_{\hat{\theta}_1}$, where $\hat{\Sigma}_{\hat{\theta}_1}$ is the inverse of the estimated Fisher information matrix. Asymptotic normality will be denoted by $\sqrt{n}(\hat{\theta}_1 - \theta_{1,0}) \dot{\sim} \mathcal{N}(\mathbf{0}, \hat{\Sigma}_{\hat{\theta}_1})$ hereafter. See Meeker and Escobar (1998) for more details on the asymptotic distribution of MLEs for the Weibull distribution.

For the inverse Gaussian distribution, the log-likelihood function is defined by

$$\begin{aligned}\mathcal{L}_{\mathrm{IG}}(\mu,\kappa) &= \sum_{i=1}^{n} \ln f_{\mathrm{IG}}(x_i;\mu,\kappa) \\ &= \frac{n}{2}\ln\left(\frac{\kappa}{2\pi}\right) - \sum_{i=1}^{n}\left\{\frac{3}{2}\ln x_i + \frac{\kappa}{2\mu^2}\frac{(x_i-\mu)^2}{x_i}\right\},\end{aligned} \quad (6)$$

and the MLEs of $\theta_2 \equiv (\mu,\kappa)$, $\hat{\theta}_2 \equiv (\hat{\mu},\hat{\kappa})$ are obtained by $\hat{\mu} \equiv \bar{x} = \sum_{i=1}^{n} x_i/n$, and $\hat{\kappa}^{-1} = \sum_{i=1}^{n}(x_i^{-1} - \bar{x}^{-1})/n$. It should be noted that $\bar{x}$ and $\sum_{i=1}^{n}(x_i^{-1} - \bar{x}^{-1})$ are independent, $\hat{\mu}$ has an inverse Gaussian distribution with mean μ and scale parameter $n\kappa$, and $n\kappa/\hat{\kappa}$ has a chi-square distribution with $(n-1)$ degrees of freedom. The MLEs of the parameters in the inverse Gaussian distribution, $\hat{\theta}_2 \xrightarrow{\text{a.s.}} \theta_{2,0} \equiv (\mu_0,\kappa_0)$ as $n\to\infty$ under no model mis-specification, where (μ_0,κ_0) are the values satisfying the following condition:

$$E_{M_2}(\mathcal{L}_{\mathrm{IG}}(\mu_0,\kappa_0)) = \max_{\tilde{\mu},\tilde{\kappa}} E_{M_2}(\mathcal{L}_{\mathrm{IG}}(\tilde{\mu},\tilde{\kappa})). \quad (7)$$

Similarly, $\sqrt{n}(\hat{\theta}_2 - \theta_{2,0}) \dot{\sim} \mathcal{N}(\mathbf{0}, \hat{\Sigma}_{\hat{\theta}_2})$, where $\hat{\Sigma}_{\hat{\theta}_2}$ is the inverse of the estimated Fisher information matrix for the inverse Gaussian distribution. See Chhikara and Folks (1989) for more details on the convergence properties of MLEs for the inverse Gaussian distribution.

2.2. *Asymptotic results of quasi-MLEs under model mis-specification*

In this section, the results in White (1982a) are used to derive the asymptotic distribution of the MLEs when the assumed model is incorrect. These incorrect MLEs were referred to as Quasi-MLEs (QMLEs) by White (1982a) (true estimators under no model mis-specification will be referred to as MLEs hereafter). The primary concern here is the accuracy and precision of failure-time characteristics when a distribution is wrongly fitted.

Let M_i and M_j be the correct model and (wrongly) fitted model, respectively. Let $\mathcal{L}(\theta_i)$ and $\mathcal{L}(\theta_j)$ be the log-likelihood function under model M_i and M_j, respectively. When the true distribution is unknown, the MLE is a natural estimator for the parameters that minimize the Kullback–Leibler Information Criterion (KLIC; see Kullback and Leibler (1951))

$$I(\theta_i,\theta_j) = E_{M_i}(\mathcal{L}(\theta_i) - \mathcal{L}(\theta_j)). \quad (8)$$

The KLIC measures the difference between the correct model and the fitted model under model mis-specification. For a fixed θ_i, let θ_j^* be the value of θ_j that minimizes $I(\theta_i,\theta_j)$ over all θ_j with respect to M_i; that is,

$\theta_j^* = \arg\min_{\theta_j}\,[I(\theta_i, \theta_j)]$. Because $E_{M_i}(\mathcal{L}(\theta_i))$ does not depend on θ_j, the value θ_j^* can be obtained by

$$\theta_j^* = \arg\min_{\theta_j}\,[E_{M_i}(-\mathcal{L}(\theta_j))].$$

Note that θ_j^* is a function of θ_i. Assuming that the true model is a Weibull distribution, the expected value of the negative log-likelihood with respect to M_1 is

$$E_{M_1}(-\mathcal{L}(\theta_2)) \propto -\frac{n}{2}\ln\kappa - \frac{n\kappa}{\mu} + \sum_{i=1}^{n}\left\{\frac{3}{2}E_{M_1}(\ln x_i) + \frac{\kappa}{2\mu^2}E_{M_1}(x_i) + \frac{\kappa}{2}E_{M_1}\left(x_i^{-1}\right)\right\},$$

for $\theta_2 \equiv (\mu, \kappa)$. It can be easily shown that

$$E_{M_1}(\ln x_i) = -\ln\lambda - \gamma/\beta, \quad E_{M_1}(x_i) = \frac{1}{\lambda\beta}\Gamma\left(\frac{1}{\beta}\right), \text{ and } E_{M_1}\left(x_i^{-1}\right) = \lambda\Gamma\left(1-\frac{1}{\beta}\right),$$

where $\gamma = -\psi(1) \approx 0.5772$ is Euler's constant and where $\psi(x) \equiv (\mathrm{d}/\mathrm{d}x)\ln\Gamma(x)$ is the digamma function. Hence, $E_{M_1}(-\mathcal{L}(\theta_2))$ can be simplified to

$$E_{M_1}(-\mathcal{L}(\theta_2)) \propto \frac{n}{2}\left(\frac{\kappa}{\mu^2\lambda\beta}\Gamma\left(\frac{1}{\beta}\right) + \lambda\kappa\Gamma\left(1-\frac{1}{\beta}\right) - \frac{2\kappa}{\mu} - \ln\kappa - 3\ln\lambda - \frac{3\gamma}{\beta}\right).$$

$\theta_2^* \equiv (\mu^*, \kappa^*)$ are obtained by solving the following equations:

$$\begin{aligned}\frac{\partial E_{M_1}(-\mathcal{L}(\theta_2))}{\partial\mu} &= -\frac{2\kappa}{\mu^3\lambda\beta}\Gamma\left(\frac{1}{\beta}\right) + \frac{2\kappa}{\mu^2} = 0,\\ \frac{\partial E_{M_1}(-\mathcal{L}(\theta_2))}{\partial\kappa} &= \frac{1}{\mu^2\lambda\beta}\Gamma\left(\frac{1}{\beta}\right) + \lambda\Gamma\left(1-\frac{1}{\beta}\right) - \frac{2}{\mu} - \frac{1}{\kappa} = 0.\end{aligned} \tag{9}$$

The resulting solution to the QMLEs in Equation (9) is

$$(\mu^*, \kappa^*) = \left(\frac{1}{\lambda\beta}\Gamma\left(\frac{1}{\beta}\right), \lambda^{-1}\left(\Gamma\left(1-\frac{1}{\beta}\right) - \beta\Gamma\left(\frac{1}{\beta}\right)^{-1}\right)^{-1}\right). \tag{10}$$

Inversely, assuming that the true model is an inverse Gaussian distribution, the expected value of the negative log-likelihood with respect to M_2 is

$$E_{M_2}(-\mathcal{L}(\theta_1)) = -n\ln\beta - n\beta\ln\lambda + \sum_{i=1}^{n}\{(\beta-1)E_{M_2}(\ln x_i) - \lambda^{\beta}E_{M_2}\left(x_i^{\beta}\right)\}.$$

Similarly, $\theta_1^* \equiv (\lambda^*, \beta^*)$ are obtained as solutions of the following equations:

$$\begin{aligned}&\frac{\partial E_{M_2}(-\mathcal{L}(\theta_1))}{\partial\lambda}\Big|_{\theta_1=\theta_1^*} = -\frac{n\beta^*}{\lambda^*} - \beta^*\lambda^{*\beta^*-1}\sum_{i=1}^{n}E_{M_2}\left(x_i^{\beta^*}\right) = 0,\\ &\frac{\partial E_{M_2}(-\mathcal{L}(\theta_1))}{\partial\beta}\Big|_{\theta_1=\theta_1^*} = -\frac{n}{\beta^*} - n\ln\lambda^* + \sum_{i=1}^{n}\left\{E_{M_2}(\ln x_i) - \lambda^{*\beta^*}\ln\lambda^* E_{M_2}\left(x_i^{\beta^*}\right) - \lambda^{*\beta^*}\frac{\partial E_{M_2}\left(x_i^{\beta}\right)}{\partial\beta}\Big|_{\beta=\beta^*}\right\} = 0,\end{aligned} \tag{11}$$

where $E_{M_2}(\ln x) = \int_0^\infty \ln x \cdot f_{\mathrm{IG}}(x;\mu,\kappa)\,\mathrm{d}x$, and $E_{M_2}(x^\beta) = \int_0^\infty x^\beta \cdot f_{\mathrm{IG}}(x;\mu,\kappa)\,\mathrm{d}x$. Obviously, there is no closed-form solution to the QMLEs in Equation (11), and these equations must be solved numerically.

Let us define the following 2×2 matrices:

$$\mathbf{A}(\theta_i : \theta_j) = \left[E_{M_i}\left(\frac{\partial^2\mathcal{L}(\theta_j)}{\partial\theta_{jr}\partial\theta_{js}}\right)\right],$$
$$\mathbf{B}(\theta_i : \theta_j) = \left[E_{M_i}\left(\frac{\partial\mathcal{L}(\theta_j)}{\partial\theta_{jr}}\frac{\partial\mathcal{L}(\theta_j)}{\partial\theta_{js}}\right)\right],$$

and

$$\mathbf{C}(\theta_i : \theta_j) = \mathbf{A}(\theta_i : \theta_j)^{-1}\,\mathbf{B}(\theta_i : \theta_j)\,\mathbf{A}(\theta_i : \theta_j)^{-1}, \tag{12}$$

where θ_{jr} is the rth element of θ_j. Note that if there is no model mis-specification (i.e., $i = j$), $-\mathbf{A}(\theta_i : \theta_i)$ is the usual Fisher information matrix. The detailed expression of $\mathbf{A}(\theta_i : \theta_j)$ and $\mathbf{B}(\theta_i : \theta_j)$ for $i, j = 1, 2$ are relegated to Appendix A. With model M_i as the true model, let $\hat{\theta}_j$ be the QMLEs when model M_j is fitted to a data set of size n. By Theorem 1 in White (1982b), $\hat{\theta}_1 \equiv (\hat{\lambda}, \hat{\beta}) \xrightarrow{\text{a.s.}} (\lambda^*, \beta^*)$, and $\hat{\theta}_2 \equiv (\hat{\mu}, \hat{\kappa}) \xrightarrow{\text{a.s.}} (\mu^*, \kappa^*)$ as $n \to \infty$ under model mis-specification. In addition, by Theorem 3.2 in White (1982a), $\sqrt{n}(\hat{\theta}_j - \theta_j^*)$ is asymptotically normal with a mean of $\mathbf{0}$ and an Asymptotic Variance–Covariance (AVCV) matrix of $\mathbf{C}(\theta_i : \theta_j = \theta_j^*)$ for $i \neq j$, $i, j = 1, 2$.

2.3. *Asymptotic properties of the functions of QMLEs*

Suppose that the main objective is to estimate a function of the parameters, which is denoted by h. The exact form of h will vary across the assumed models. In this section, we address the effect of model mis-specification on the accuracy and precision of the failure-time characteristics of interest such as quantiles and MTTF. Let $h_j(\theta_j)$ denote h under M_j for $j = 1, 2$. By the invariance property, $h_j(\hat{\theta}_j)$ is the QMLE of h under the mis-specified model M_j, and is asymptotically normal with an asymptotic mean $h_j(\theta_j^*)$

and Asymptotic Variance (AVAE):

$$\text{AVAR}\left(h_j(\hat{\boldsymbol{\theta}}_j)|M_i\right) = \frac{1}{n}\left(\frac{\partial h_j(\boldsymbol{\theta}_j)}{\partial \boldsymbol{\theta}_j}\Big|_{\boldsymbol{\theta}_j=\boldsymbol{\theta}_j^*}\right)^{\mathrm{T}} \mathbf{C}(\boldsymbol{\theta}_i : \boldsymbol{\theta}_j = \boldsymbol{\theta}_j^*)\left(\frac{\partial h_j(\boldsymbol{\theta}_j)}{\partial \boldsymbol{\theta}_j}\Big|_{\boldsymbol{\theta}_j=\boldsymbol{\theta}_j^*}\right). \tag{13}$$

For instance, suppose that the population MTTF is of interest. Let $\widehat{MTTF}_2$ denote the QMLE of the MTTF when the true model is M_1. The QMLE of the $MTTF_2$ is $\widehat{MTTF}_2 \equiv \hat{\mu} = \bar{x}$. Then, using the KLIC to measure the difference between the correct model (Weibull distribution) and the fitted model (inverse Gaussian distribution), we obtain the following result.

Theorem 1.

$$\widehat{MTTF}_2 \dot{\sim} \mathcal{N}\left(MTTF_1, \frac{c_{11}}{n}\right),$$

where $MTTF_1 = (\lambda\beta)^{-1}\Gamma(1/\beta)$ *and* c_{11} *is the* $(1,1)$*th element of the AVCV matrix* $\mathbf{C}(\boldsymbol{\theta}_1 : \boldsymbol{\theta}_2 = \boldsymbol{\theta}_2^*)$.

Proof. The proof follows immediately from Equations (10) and (13).

Next, we are interested in the asymptotic distribution for the QMLE of the MTTF for the Weibull distribution when the true model is the inverse Gaussian distribution. Let $\widehat{MTTF}_1$ denote the QMLE of the MTTF when the true model is M_2. The QMLE of the $MTTF_1$ is $\widehat{MTTF}_1 = \hat{\lambda}^{-1}\Gamma(1 + 1/\hat{\beta})$. This yields the following result. ■

Result 1.

$$\widehat{MTTF}_1 \dot{\sim} \mathcal{N}\left(\frac{1}{\lambda^*}\Gamma\left(1+\frac{1}{\beta^*}\right), \frac{1}{n}\mathbf{U}\mathbf{C}(\boldsymbol{\theta}_2 : \boldsymbol{\theta}_1 = \boldsymbol{\theta}_1^*)\mathbf{U}^{\mathrm{T}}\right),$$

where λ^* and β^* are derived by solving Equation (11), $\mathbf{C}(\boldsymbol{\theta}_2 : \boldsymbol{\theta}_1 = \boldsymbol{\theta}_1^*)$ is derived via $\mathbf{A}(\boldsymbol{\theta}_2 : \boldsymbol{\theta}_1 = \boldsymbol{\theta}_1^*)$ and $\mathbf{B}(\boldsymbol{\theta}_2 : \boldsymbol{\theta}_1 = \boldsymbol{\theta}_1^*)$ in Appendix A, and

$$\mathbf{U} = \left(\frac{\partial MTTF_1}{\partial\lambda}, \frac{\partial MTTF_1}{\partial\beta}\right)\Big|_{\boldsymbol{\theta}_1=\boldsymbol{\theta}_1^*} = \left(-\frac{1}{\lambda^{*2}}\Gamma\left(1+\frac{1}{\beta^*}\right), -\frac{1}{\lambda^*\beta^{*2}}\Gamma'\left(1+\frac{1}{\beta^*}\right)\right).$$

Its proof follows from $h_1(\hat{\boldsymbol{\theta}}_1) \xrightarrow{\text{a.s.}} h_1(\boldsymbol{\theta}_1^*)$ as $n \to \infty$, $\widehat{MTTF}_1 \xrightarrow{\text{a.s.}} \lambda^{*-1}\Gamma(1 + 1/\beta^*)$, and the asymptotic variance for $\widehat{MTTF}_1$ results from Equation (13).

Let $\hat{y}_{1,p}$ denote the QMLE of the pth quantile when the true model is M_2. The QMLE of $y_{1,p}$ is $\hat{y}_{1,p} = \hat{\lambda}^{-1}[-\ln(1-p)]^{1/\hat{\beta}}$. This yields the following result.

Result 2.

$$\hat{y}_{1,p} \dot{\sim} \mathcal{N}\left(\frac{1}{\lambda^*}[-\ln(1-p)]^{1/\beta^*}, \times \frac{1}{n}\mathbf{V}\mathbf{C}(\boldsymbol{\theta}_2 : \boldsymbol{\theta}_1 = \boldsymbol{\theta}_1^*)\mathbf{V}^{\mathrm{T}}\right),$$

where

$$\mathbf{V} = \left(\frac{\partial y_{1,p}}{\partial\lambda}, \frac{\partial y_{1,p}}{\partial\beta}\right)\Big|_{\boldsymbol{\theta}_1=\boldsymbol{\theta}_1^*} = \left(-\frac{1}{\lambda^{*2}}[-\ln(1-p)]^{1/\beta^*}, -\frac{\ln(-\ln(1-p))}{\lambda^*\beta^{*2}} \times [-\ln(1-p)]^{1/\beta^*}\right).$$

Let $\text{Bias}(h_j(\hat{\boldsymbol{\theta}}_j)|M_i)$ denote the approximate bias of $h_j(\hat{\boldsymbol{\theta}}_j)$ as an estimate of $h_i(\boldsymbol{\theta}_i)$ when the true model is M_i. The observed bias

$$\text{Bias}(h_j(\hat{\boldsymbol{\theta}}_j)|M_i) = h_j(\hat{\boldsymbol{\theta}}_j) - h_i(\boldsymbol{\theta}_i) \tag{14}$$

is asymptotically normal with an asymptotic mean and asymptotic variance, respectively, of

$$\text{ABias}\left(h_j(\boldsymbol{\theta}_j^*)|M_i\right) = h_j(\boldsymbol{\theta}_j^*) - h_i(\boldsymbol{\theta}_i), \text{ and}$$
$$\text{AVAR}\left(\text{ABias}(h_j(\boldsymbol{\theta}_j^*)|M_i)\right) = \text{AVAR}\left(h_j(\hat{\boldsymbol{\theta}}_j)|M_i\right). \tag{15}$$

Note that $\text{AVAR}\left(\text{ABias}(h_j(\boldsymbol{\theta}_j^*)|M_i)\right)$ depends on $\boldsymbol{\theta}_i$ and the sample size n, whereas $\text{ABias}(h_j(\boldsymbol{\theta}_j^*)|M_i)$ depends on $\boldsymbol{\theta}_i$ but not on n. Let us define the Asymptotic Mean Squared Error (AMSE) of the QMLE $h_j(\hat{\boldsymbol{\theta}}_j)$ to estimate the correct $h_i(\boldsymbol{\theta}_i)$ by

$$\begin{aligned}\text{AMSE}[h_j(\hat{\boldsymbol{\theta}}_j)|M_i] &= \lim_{n\to\infty} E_{M_i}\{(h_j(\hat{\boldsymbol{\theta}}_j) - h_i(\boldsymbol{\theta}_i))^2\} \\ &= \text{AVAR}(h_j(\hat{\boldsymbol{\theta}}_j)|M_i) \\ &\quad + \{\text{ABias}(h_j(\boldsymbol{\theta}_j^*)|M_i)\}^2. \end{aligned} \tag{16}$$

Then, by Theorem 1, $\text{AVAR}[\widehat{MTTF}_2|M_1] \to 0$ and $\text{AMSE}[\widehat{MTTF}_2|M_1] \to 0$ for a large n.

3. Discrimination between Weibull and inverse Gaussian distributions

In this section, the PCS is computed to discriminate between the Weibull and inverse Gaussian distributions, based on the asymptotic distribution of the RML. The RML has been used to discriminate between pairs of overlapping families of distributions: Weibull and generalized exponential distributions (Gupta and Kundu, 1951), Weibull and lognormal distributions (Kundu and Manglick, 2004), and lognormal and generalized exponential distributions (Kundu and Manglick, 2005). Kundu and Manglick (2004) showed that the asymptotic distribution

of the RML under the Weibull and lognormal distributions is normal and independent of unknown parameters. They also used the PCS to determine the minimum sample size required to discriminate between the Weibull and lognormal distributions.

3.1. *Asymptotic distribution of likelihood ratio statistics*

For the Weibull log-likelihood (4) and the inverse Gaussian log-likelihood (6), the logarithm of the RML is defined as

$$Q = \mathcal{L}_{\mathrm{IG}}(\hat{\boldsymbol{\theta}}_2) - \mathcal{L}_{\mathrm{WE}}(\hat{\boldsymbol{\theta}}_1) \equiv \mathcal{L}_{\mathrm{IG}}(\hat{\mu}, \hat{\kappa}) - \mathcal{L}_{\mathrm{WE}}(\hat{\lambda}, \hat{\beta}),$$

where $(\hat{\lambda}, \hat{\beta})$ and $(\hat{\mu}, \hat{\kappa})$ are the respective MLEs of (λ, β) and (μ, κ), based on the samples $x_1, \ldots, x_n$. The logarithm of the RML can be written as

$$\begin{aligned} Q = {} & \hat{\lambda}^{\hat{\beta}} \sum_{i=1}^{n} x_i^{\hat{\beta}} - \left(\frac{1}{2} + \hat{\beta}\right) \tilde{x} + n \ln\left(\frac{\hat{\kappa}^{1/2}}{\hat{\beta}\hat{\lambda}^{\hat{\beta}}}\right) \\ & - \frac{n}{2}\left(\ln(2\pi) + 1\right), \end{aligned} \tag{17}$$

where $\tilde{x} = \sum_{i=1}^{n} \ln x_i$. We choose the inverse Gaussian if the test statistic $Q > 0$; otherwise, we choose the Weibull distribution as the preferred model (Kundu and Manglick, 2004).

Let $Q^* = \mathcal{L}_{\mathrm{IG}}(\mu^*, \kappa^*) - \mathcal{L}_{\mathrm{WE}}(\lambda_0, \beta_0)$, where (λ_0, β_0) are true values of (λ, β) that satisfy Equation (5). Suppose that the true distribution is the Weibull (M_1); then, by Theorem 1 in White (1982b), $n^{-1/2}(Q - E_{M_1}(Q))$ is asymptotically equivalent in distribution to $n^{-1/2}(Q^* - E_{M_1}(Q^*))$, where $E_{M_1}(Q)$ and $E_{M_1}(Q^*)$ are the mean of Q and the mean of Q^* under the correct model M_1, respectively. By defining the variance of Q as $\mathrm{VAR}_{M_1}(Q)$, Q is asymptotically normally distributed with a mean of $E_{M_1}(Q)$ and variance of $\mathrm{VAR}_{M_1}(Q)$ because $n^{-1/2}(Q^* - E_{M_1}(Q^*))$ is asymptotically normally distributed. Denote $\lim_{n\to\infty}[E_{M_1}(Q)/n] = \mathrm{AM}_{M_1}$ and $\lim_{n\to\infty}[\mathrm{VAR}_{M_1}(Q)/n] = \mathrm{AVAR}_{M_1}$, then AM_{M_1} and AVAR_{M_1} exist. For a large n:

$$\begin{aligned} \frac{E_{M_1}(Q)}{n} &\simeq \mathrm{AM}_{M_1} = E_{M_1}\left(\ln f_{\mathrm{IG}}(\mu^*, \kappa^*) - \ln f_{\mathrm{WE}}(\lambda_0, \beta_0)\right) \\ &= \frac{1}{2}\left\{-\ln \Upsilon(\beta_0) + 1 - \ln(2\pi) + \gamma\left(2 + \frac{1}{\beta_0}\right)\right\} \\ &\quad - \ln \beta_0, \end{aligned} \tag{18}$$

where $\Upsilon(\beta_0) = \Gamma(1 - 1/\beta_0) - \beta_0 \Gamma(1/\beta_0)^{-1}$. The derivation of Equation (18) is detailed in Appendix B. Note that the approximated mean of Q is independent of the Weibull scale parameter λ and only depends on the shape parameter β. For a large n:

$$\begin{aligned} \frac{\mathrm{VAR}_{M_1}(Q)}{n} &\simeq \mathrm{AVAR}_{M_1} = \mathrm{VAR}_{M_1}\big(\ln f_{\mathrm{IG}}(\mu^*, \kappa^*) \\ &\quad - \ln f_{\mathrm{WE}}(\lambda_0, \beta_0)\big). \end{aligned}$$

By letting $y = \lambda x$, y has a Weibull distribution with a scale parameter of one and shape parameter of β, and

$$\begin{aligned} \mathrm{AVAR}_{M_1} = {} & \mathrm{VAR}\Bigg(-\frac{1}{2}\frac{\kappa^*}{\lambda_0 \mu^{*2}} y - \frac{\lambda_0 \kappa^*}{2} y^{-1} - \left(\beta_0 + \frac{1}{2}\right) \\ & \times \ln y + y^{\beta_0}\Bigg) \\ = {} & \frac{\kappa^{*2}}{4\lambda_0^2 \mu^{*4}}\left(\Gamma\left(1 + \frac{2}{\beta_0}\right) - \Gamma\left(1 + \frac{1}{\beta_0}\right)^2\right) \\ & + \frac{\lambda_0^2 \kappa^{*2}}{4}\left(\Gamma\left(1 - \frac{2}{\beta_0}\right) - \Gamma\left(1 - \frac{1}{\beta_0}\right)^2\right) \\ & + \left(\beta_0 + \frac{1}{2}\right)^2 \frac{\psi'(1)}{\beta_0^2} + 1 + \frac{\kappa^*}{\lambda_0 \mu^{*2}}\left(1 + \frac{1}{2\beta_0}\right) \\ & \times \left(\psi\left(1 + \frac{1}{\beta_0}\right)\Gamma\left(1 + \frac{1}{\beta_0}\right) - \Gamma\left(1 + \frac{1}{\beta_0}\right)\right. \\ & \left. \times \psi(1)\right) + \kappa^* \lambda_0 \left(1 + \frac{1}{2\beta_0}\right)\left(\psi\left(1 - \frac{1}{\beta_0}\right)\right. \\ & \left. \times \Gamma\left(1 - \frac{1}{\beta_0}\right) - \Gamma\left(1 - \frac{1}{\beta_0}\right)\psi(1)\right) \\ & - 2\left(1 + \frac{1}{2\beta_0}\right)(\psi(2) - \psi(1)) + \frac{\kappa^{*2}}{2\mu^{*2}} \\ & \times \left(1 - \Gamma\left(1 + \frac{1}{\beta_0}\right)\Gamma\left(1 - \frac{1}{\beta_0}\right)\right) \\ & - \frac{\kappa^*}{\mu^{*2}\lambda_0}\left(\Gamma\left(1 + \frac{\beta_0 + 1}{\beta_0}\right) - \Gamma\left(1 + \frac{1}{\beta_0}\right)\right) \\ & - \kappa^* \lambda_0 \left(\Gamma\left(1 + \frac{\beta_0 - 1}{\beta_0}\right) - \Gamma\left(1 - \frac{1}{\beta_0}\right)\right), \end{aligned} \tag{19}$$

where $\psi'(x) \equiv (\mathrm{d}/\mathrm{d}x)\psi(x)$ is the polygamma function.

Similarly, denote $\lim_{n\to\infty}[E_{M_2}(Q)/n] = \mathrm{AM}_{M_2}$ and $\lim_{n\to\infty}[\mathrm{VAR}_{M_2}(Q)/n] = \mathrm{AVAR}_{M_2}$. Under the existence of AM_{M_2} and AVAR_{M_2}, for a large n:

$$\begin{aligned} \frac{E_{M_2}(Q)}{n} &\simeq \mathrm{AM}_{M_2} = E_{M_2}\big(\ln f_{\mathrm{IG}}(\mu_0, \kappa_0) \\ &\quad - \ln f_{\mathrm{WE}}(\lambda^*, \beta^*),\big), \\ \frac{\mathrm{VAR}_{M_2}(Q)}{n} &\simeq \mathrm{AVAR}_{M_2} = \mathrm{VAR}_{M_2}\big(\ln f_{\mathrm{IG}}(\mu_0, \kappa_0) \\ &\quad - \ln f_{\mathrm{WE}}(\lambda^*, \beta^*)\big). \end{aligned} \tag{20}$$

AM_{M_2} and AVAR_{M_2} can be obtained numerically after plugging λ^* and β^* into Equation (20).

3.2. *Computation of the PCS*

In the previous section, we noted that the logarithm of the RML is $Q \dot{\sim} \mathcal{N}(E_{M_1}(Q), \mathrm{VAR}_{M_1}(Q))$. The aymptotic mean and variance of Q can be approximated via the mean and variance of Q^* by using asymptotic equivalence in

distribution. The PCS is approximated by

$$\mathrm{PCS} = \Pr[Q < 0] \approx \Phi\left[-\frac{E_{M_1}(Q)}{\sqrt{\mathrm{VAR}_{M_1}(Q)}}\right] \simeq 1 - \Phi\left(\frac{n \cdot \mathrm{AM}_{M_1}}{\sqrt{n \cdot \mathrm{AVAR}_{M_1}}}\right). \quad (21)$$

The PCS can be used for hypothesis test of

H_0 : Weibull versus H_1 : Inverse Gaussian.

Dumonceaux and Antle (1973) provided the exact critical regions and the powers of the likelihood ratio tests as the discrimination problem between the lognormal and Weibull distribution, based on Monte Carlo simulations. Following the approach of Dumonceaux and Antle (1973), we reject the null hypothesis H_0 at an α-level of significance if $Q > -n \cdot \mathrm{AM}_{M_1} + z_\alpha \sqrt{n \cdot \mathrm{AVAR}_{M_1}}$ and accept it otherwise. Here, z_α is the $100(1-\alpha)$ percentile point of a standard normal distribution.

The minimum sample size needed to discriminate between Weibull and inverse Gaussian distributions can be determined for a given user-specified PCS. The PCS is assumed to be specified by the user in advance. At the least p^* protection level, the minimum sample size is derived by equating

$$\Phi\left(\frac{n \cdot \mathrm{AM}_{M_1}}{\sqrt{n \cdot \mathrm{AVAR}_{M_1}}}\right) = 1 - p^*$$

and obtaining

$$n = \frac{z_{p^*}^2 \cdot \mathrm{AVAR}_{M_1}}{(\mathrm{AM}_{M_1})^2}, \quad (22)$$

where z_{p^*} is the $100(1-p^*)$ percentile point of a standard normal distribution.

4. Shock test data for SMP display modules

We conducted shock tests after mounting SMP display modules on the carriage of a shock test machine. The shock test machine must have a flat horizontal test surface (carriage) with sufficient strength and rigidity to remain flat and horizontal under the stresses that develop during the shock test. A damaged SMP display module can render the product unacceptable because it fails to meet performance specifications. The fragility of a product is specified by the DBC. The DBC, shown in Fig. 1, mainly consists of the critical acceleration (A_c) and the critical velocity change (V_c).

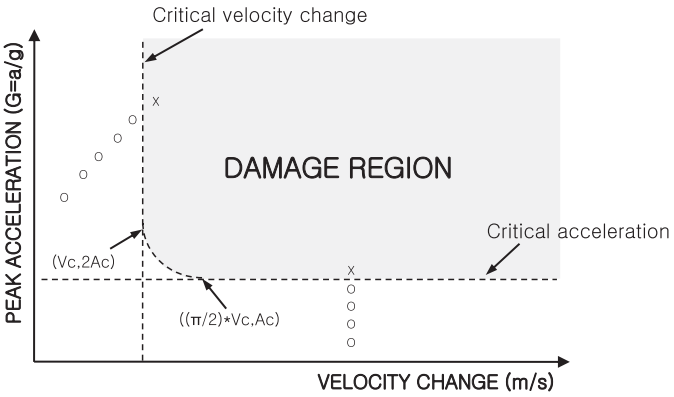

Fig. 1. A DBC (○: non-failure, ×: failure).

Critical acceleration is obtained by regularly increasing the drop height of the carriage to which the SMP display module is mounted at fixed velocity change until failure occurs. The velocity change is adjusted using a number of cushioning layers that decrease the severity of the shock delivered to the carriage. The critical velocity change is determined by eliminating the cushioning layers one at a time at a fixed drop height until failure occurs. In this experiment, 14 SMP display modules were used for the critical acceleration test and an additional 14 were used for the critical velocity change test. The shock test results are given in Table 1.

The Weibull and inverse Gaussian distributions were fitted to the critical acceleration test data of the SMP display modules. MLEs of the parameters, along with corresponding log-likelihood value are summarized in Table 2. As a measure of goodness-of-fit, the Kolmogorov–Smirnov (K–S) distance between the data and the fitted distribution was calculated. The K–S distance for the fitted Weibull distribution is 0.2484 with a corresponding p-value of 0.3011, and the K–S distance for the fitted inverse Gaussian distribution is 0.2260, with a corresponding p-value of 0.4108. We also fitted the critical velocity change data of the SMP display modules to the Weibull and inverse Gaussian distributions and resulting MLEs of the parameters, along with corresponding log-likelihood value, which are also presented in Table 2. The K–S distance between the data and the fitted Weibull distribution is 0.2188 with a corresponding p-value of 0.5143. In contrast, the K–S distance between the data and the fitted inverse Gaussian distribution is 0.1947 with a corresponding p-value of 0.6637.

Weibull and inverse Gaussian survival functions were fitted to the critical acceleration and critical velocity change data and are individually plotted in Fig. 2, along with a

Table 1. Shock failure data for SMP display modules evaluated using the critical acceleration test ($n = 14$) and the critical velocity change test ($n = 14$)

A_c $^{(\times 10^3)}$	5.396 6.076 6.083 6.173 6.240 6.333 6.543 6.720 8.203 8.520 8.756 8.933 9.503 10.500
V_c	4.967 4.967 5.214 5.459 5.459 5.459 5.459 5.702 5.702 5.702 5.702 5.702 5.944 6.184

Table 2. MLEs of the Weibull and inverse Gaussian distribution

	Weibull			*Inverse Gaussian*		
	$(\hat{\lambda}, \hat{\beta})$	$\mathcal{L}_{WE}$	*K–S (p-value)*	$(\hat{\mu}, \hat{\kappa})$	$\mathcal{L}_{IG}$	*K–S (p-value)*
A_c	(0.1240, 5.1585)	−26.2447	0.2484 (0.3011)	(7.4276, 181.79)	−25.1219	0.2260 (0.4108)
V_c	(0.1755, 18.4606)	−4.5963	0.2188 (0.5143)	(5.5442, 1563.1943)	−4.3157	0.1947 (0.6637)

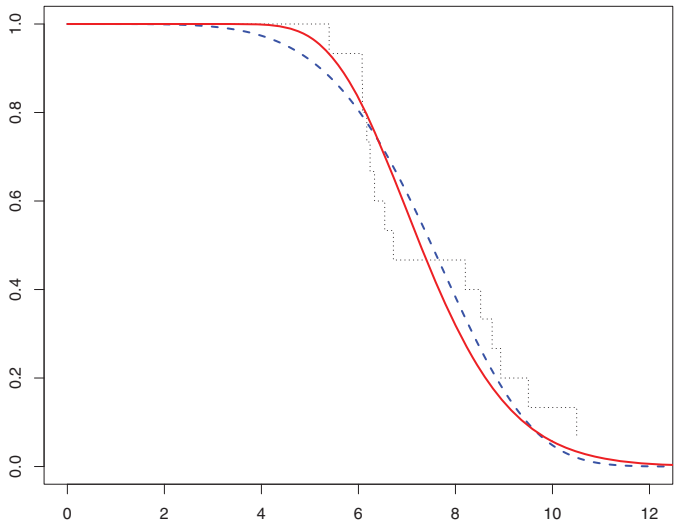

(a)

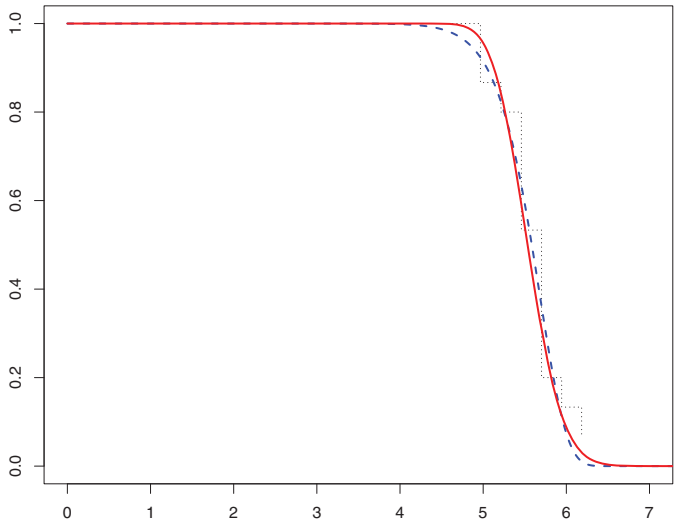

(b)

Fig. 2. Fitting of a nonparametric survival function, Weibull, and inverse Gaussian survival functions to (a) the critical acceleration data and (b) the critical velocity change data of the SMP display modules (⋯ nonparametric, - - - Weibull, — inverse Gaussian).

nonparametric survival function for comparison. The K–S distances and Fig. 2 indicate that both the Weibull and inverse Gaussian distributions provide a good fit to the critical acceleration and critical velocity change test data.

In comparison with the logarithmic value of RML, $Q_{A_c} = -25.1219 + 26.2447 = 1.1228 > 0$ for the critical acceleration test data (see Table 3). To compute the PCS to identify the better distribution, when we assumed that the true distribution was a Weibull, the PCS is 0.7196 based on a sample size of 14. To test the hypothesis H_0: Weibull versus H_1: inverse Gaussian, $Q_{A_c} < 14 \cdot 0.0984 + 1.645\sqrt{14 \cdot 0.4008} = 3.4605$; thus, the null hypothesis of a Weibull distribution was not rejected at the significance level $\alpha = 0.05$. In contrast, when we assumed that the true distribution was an inverse Gaussian, the PCS was 0.7495. To test hypothesis H_0: inverse Gaussian versus H_1: Weibull, $Q_{A_c} > 14 \cdot 0.0802 - 1.645\sqrt{14 \cdot 0.1986} = -0.3434$; thus, the null hypothesis of the inverse Gaussian distribution was not rejected at the significance level $\alpha = 0.05$. In this case, the PCS was at least $\min\{0.7196, 0.7495\} = 0.7196$. When we assumed that the A_c data followed a Weibull distribution, the p-value was 0.1455, whereas when we assumed that the A_c data followed an inverse Gaussian distribution, the p-value was 0.5002. The Q value, K–S distances, and p-values indicate that the inverse Gaussian distribution best describes the data, and the probability of correct selection is at least 71.96% for the critical acceleration data. The minimum sample size required to achieve an overall p^* protection level is

$$n_{A_c} = z_{p^*}^2 \max\left\{\frac{\mathrm{AVAR}_{M_1,A_c}}{(\mathrm{AM}_{M_1,A_c})^2}, \frac{\mathrm{AVAR}_{M_2,A_c}}{(\mathrm{AM}_{M_2,A_c})^2}\right\} = z_{p^*}^2 \max\{41.3940, 30.8767\} = 41.3940 \cdot z_{p^*}^2.$$

The minimum sample sizes required to discriminate between Weibull and inverse Gaussian distribution for each p^* protection level are indicated in Table 4.

For the critical velocity change test data, $Q_{V_c} = -4.3157 + 4.5963 = 0.2807 > 0$. To compute the PCS to

Table 3. PCS of the Weibull and inverse Gaussian distribution

	Weibull			*Inverse Gaussian*			
	AM_{M_1}	$AVAR_{M_1}$	*PCS*	AM_{M_2}	$AVAR_{M_2}$	*PCS*	Q
A_c	−0.0984	0.4008	0.7196	0.0802	0.1986	0.7495	1.1228
V_c	−1.4137	0.6337	≈ 1.00	0.0893	0.2163	0.7425	0.2807

Table 4. Minimum sample size required for each p^* protection level

	p^*			
	0.6	*0.7*	*0.8*	*0.9*
A_c	2.6569	11.3832	29.3205	67.9845
V_c	2.2455	9.6205	24.7802	57.4572

identify the better fitting distribution, when we assumed that the true distribution was a Weibull, the PCS ≈ 1.00 based on a sample size of 14 (see Table 3). To test the hypothesis H_0: Weibull versus H_1: inverse Gaussian, $Q_{V_c} < 14 \cdot 1.4137 + 1.645\sqrt{14 \cdot 0.6337} = 24.6915$; thus, the null hypothesis of a Weibull distribution was not rejected at the significance level $\alpha = 0.05$. However, when we assumed that the true distribution was an inverse Gaussian, the PCS was 0.7425. To test the hypothesis H_0: inverse Gaussian versus H_1: Weibull, $Q_{V_c} > 14 \cdot 0.0893 - 1.645\sqrt{14 \cdot 0.2163} = -1.6124$; thus, the null hypothesis of an inverse Gaussian distribution was not failed rejected at the significance level $\alpha = 0.05$ for the critical velocity change test data. In this case, the PCS was at least $\min\{1.00, 0.7425\} = 0.7425$. Under the assumption that the V_c data followed a Weibull distribution, the p-value was 0.2201, whereas under the assumption that the V_c data followed the inverse Gaussian distribution, the p-value was 0.3121. The Q value, K–S distances, and p-values indicate that an inverse Gaussian distribution best fits the data, and the probability of correct selection is at least 74.25% for the critical acceleration data. The minimum sample size needed to achieve an overall p^* protection level is

$$n_{V_c} = z_{p^*}^2 \max\left\{\frac{\mathrm{AVAR}_{M_1,V_c}}{(\mathrm{AM}_{M_1,V_c})^2}, \frac{\mathrm{AVAR}_{M_2,V_c}}{(\mathrm{AM}_{M_2,V_c})^2}\right\} = z_{p^*}^2 \max\{34.9842, 33.0225\} = 34.9842 \cdot z_{p^*}^2.$$

For the critical velocity change data, the minimum sample sizes required for each p^* protection level are also shown in Table 4.

In conclusion, we chose the inverse Gaussian model as the best-fitting model for both the critical acceleration and critical velocity change data. Point estimates of the pth quantiles and MTTF with the Weibull and the inverse Gaussian distributions, along with their 95% pointwise confidence intervals (in parentheses), are shown in Table 5. Note that the confidence intervals of the inverse Gaussian estimates of the pth quantiles and MTTF are consistently narrower than those of the Weibull estimates. Figure 3 depicts the DBC based on the MLE of MTTF, along with 95% confidence bands, for when the inverse Gaussian distribution was fitted to the shock data set.

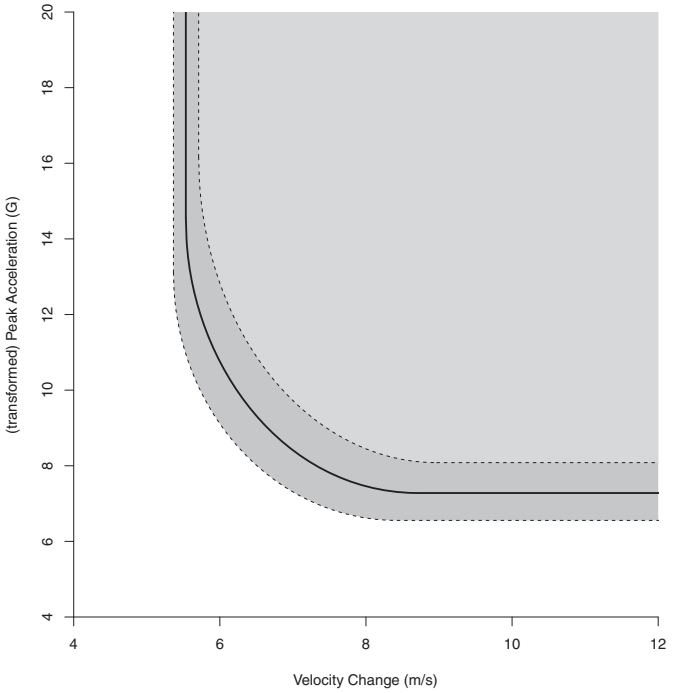

Fig. 3. The DBC based on the MLE estimate of MTTF in fitting the inverse Gaussian distribution, along with 95% confidence bands.

5. Numerical experiments

In this section, we report the results of simulation experiments that we performed to determine the PCS and

Table 5. MLE of quantiles and MTTF along with their 95% confidence intervals for the Weibull and the inverse Gaussian failure-time distributions

		Quantile					
		0.05	*0.10*	*0.50*	*0.90*	*0.95*	*MTTF*
A_c	Weibull	4.535 (3.416, 6.022)	5.214 (4.132, 6.580)	7.512 (6.662, 8.472)	9.480 (8.532, 10.534)	9.977 (8.915, 11.164)	7.403 (6.660, 8.230)
	Inverse Gaussian	5.239 (4.467, 6.145)	5.631 (4.891, 6.483)	7.279 (6.555, 8.083)	9.413 (8.171, 10.843)	10.119 8.620, 11.879)	7.427 (6.641, 8.213)
V_c	Weibull	4.850 (4.487, 5.242)	5.043 (4.731, 5.376)	5.585 (5.401, 5.774)	5.960 (5.787, 6.138)	6.045 (5.859, 6.238)	5.534 (5.345, 5.731)
	Inverse Gaussian	5.018 (4.784, 5.264)	5.128 (4.917, 5.348)	5.535 (5.365, 5.710)	5.974 (5.727, 6.230)	6.104 (5.819, 6.403)	5.544 (5.371, 5.718)

Table 6. MC simulation results for the mean and variance of the ratio of the MLE for the A_c case

	Sample size (n)				
	10	*50*	*100*	*500*	*1000*
$\bar{Q}_{M_1}$	−0.0521	−0.0866	−0.0903	−0.0970	−0.0975
VAR_{Q,M_1}	0.1283	0.2782	0.3106	0.3815	0.3890
$\bar{Q}_{M_2}$	0.0379	0.0674	0.0743	0.0785	0.0792
VAR_{Q,M_2}	0.0882	0.1429	0.1744	0.1861	0.1902

estimation precision, based on asymptotic results, for different sample sizes and for different parameter values. The PCS and estimation precision under model mis-specification depend on the parameters of the true distribution and sample size. In the analysis of critical acceleration data based on 14 samples in Section 4, $\mathrm{AM}_{M_1} = -0.0984$ ($\mathrm{AM}_{M_2} = 0.0802$) and $\mathrm{AVAR}_{M_1} = 0.4008$ ($\mathrm{AVAR}_{M_2} = 0.1986$) under the assumption that the true distribution was a Weibull (inverse Gaussian) distribution. We performed Monte Carlo (MC) simulations to examine the asymptotical properties of the RML based on $N = 10\,000$ replications. Based on the assumption that the true distribution was a Weibull (inverse Gaussian) distribution, we treated the MLEs $\hat{\theta}_1$ ($\hat{\theta}_2$) as the true parameters for θ_1 (θ_2). The mean and variance from the simulations were calculated by $\bar{Q} = \sum_{i=1}^{N} Q_i/N$, and $\mathrm{VAR}_Q = \sum_{i=1}^{N}(Q_i - \bar{Q})^2/N - 1$, respectively. Note from Table 6 that the mean and variance calculated from the MC simulations approach the theoretical asymptotic mean and asymptotic variance derived in Section 3 as the sample size increases. We computed the PCS based on both the MC simulations and the asymptotic results derived in Section 3. The parameter values for the Weibull and inverse Gaussian distributions were also based on the MLEs ($\hat{\theta}_1$, $\hat{\theta}_2$) in Section 3 in the 10 000 simulation replications. The PCS was computed as the percentage of times the correct distribution function was chosen by checking whether Q was positive or negative. These results are reported in Table 7. It is quite clear from Table 7 that the PCS increases as the sample size increases, as expected. Even for moderate sample sizes ($n = 20$), the asymptotic results match up reasonably well with the simulation results for both of these scenarios.

Table 7. The probability of correct selection based on MC simulations and the asymptotic results (AS) for the A_c case

	Sample size (n)					
	10	*20*	*40*	*60*	*80*	*100*
MC_{M_1}	0.6617	0.7623	0.8700	0.9296	0.9566	0.9735
AS_{M_1}	0.6885	0.7566	0.8373	0.8858	0.9178	0.9400
MC_{M_2}	0.6781	0.7773	0.8800	0.9266	0.9562	0.9718
AS_{M_2}	0.7153	0.7894	0.8724	0.9182	0.9462	0.9640

Table 8. PCS based on MC simulations and asymptotic results when the true distribution was a Weibull distribution for a fixed $\lambda = 0.1$. The elements of the first row in each cell represent the MC results and the numbers in parentheses represent the asymptotic results

	Sample size (n)				
β	*20*	*40*	*60*	*80*	*100*
2.5	0.7670	0.8788	0.9337	0.9591	0.9760
	(0.6668)	(0.7290)	(0.7724)	(0.8057)	(0.8325)
3	0.7686	0.8797	0.9282	0.9614	0.9751
	(0.7077)	(0.7803)	(0.8282)	(0.8629)	(0.8892)
3.5	0.7608	0.8759	0.9289	0.9564	0.9751
	(0.7289)	(0.8056)	(0.8544)	(0.8885)	(0.9135)
4	0.7708	0.8704	0.9262	0.9565	0.9712
	(0.7415)	(0.8202)	(0.8691)	(0.9025)	(0.9263)
4.5	0.7685	0.8732	0.9265	0.9578	0.9705
	(0.7496)	(0.8295)	(0.8782)	(0.9109)	(0.9339)
5	0.7660	0.8706	0.9251	0.9554	0.9722
	(0.7552)	(0.8358)	(0.8843)	(0.9165)	(0.9388)
5.5	0.7682	0.8739	0.9219	0.9539	0.9686
	(0.7592)	(0.8402)	(0.8886)	(0.9204)	(0.9422)
6	0.7718	0.8781	0.9251	0.9544	0.9690
	(0.7622)	(0.8435)	(0.8917)	(0.9232)	(0.9447)
6.5	0.7618	0.8726	0.9248	0.9540	0.9702
	(0.7644)	(0.8459)	(0.8940)	(0.9253)	(0.9465)

Table 9. PCS based on MC simulations and asymptotic results when the true distribution was an inverse Gaussian. The elements of the first row in each cell represent the MC results and the numbers in parentheses represent the asymptotic results

		Sample size (n)				
μ	κ	*20*	*40*	*60*	*80*	*100*
1.0	50	0.7785	0.8764	0.9260	0.9579	0.9725
		(0.7854)	(0.8682)	(0.9145)	(0.9431)	(0.9614)
	100	0.7691	0.8763	0.9235	0.9534	0.9712
		(0.7832)	(0.8660)	(0.9125)	(0.9414)	(0.9600)
	150	0.7708	0.8716	0.9249	0.9566	0.9711
		(0.7825)	(0.8652)	(0.9118)	(0.9408)	(0.9596)
5.0	50	0.7817	0.8823	0.9283	0.9577	0.9739
		(0.7998)	(0.8828)	(0.9274)	(0.9537)	(0.9700)
	100	0.7714	0.8766	0.9259	0.9571	0.9752
		(0.7910)	(0.8740)	(0.9197)	(0.9474)	(0.9649)
	150	0.7685	0.8797	0.9216	0.9569	0.9741
		(0.7878)	(0.8707)	(0.9168)	(0.9450)	(0.9630)
10.0	50	0.7986	0.8898	0.9410	0.9624	0.9803
		(0.8146)	(0.8972)	(0.9395)	(0.9633)	(0.9773)
	100	0.7830	0.8829	0.9322	0.9601	0.9748
		(0.7998)	(0.8828)	(0.9273)	(0.9537)	(0.9699)
	150	0.7769	0.8796	0.9345	0.9588	0.9745
		(0.7942)	(0.8772)	(0.9225)	(0.9497)	(0.9668)

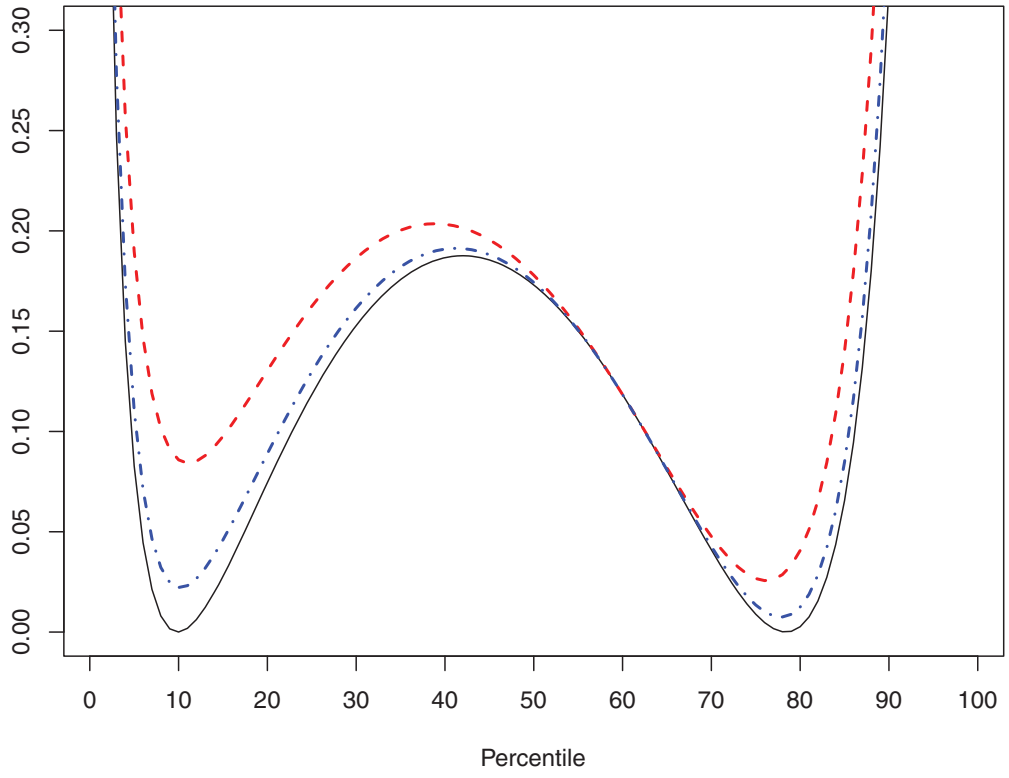

(a)

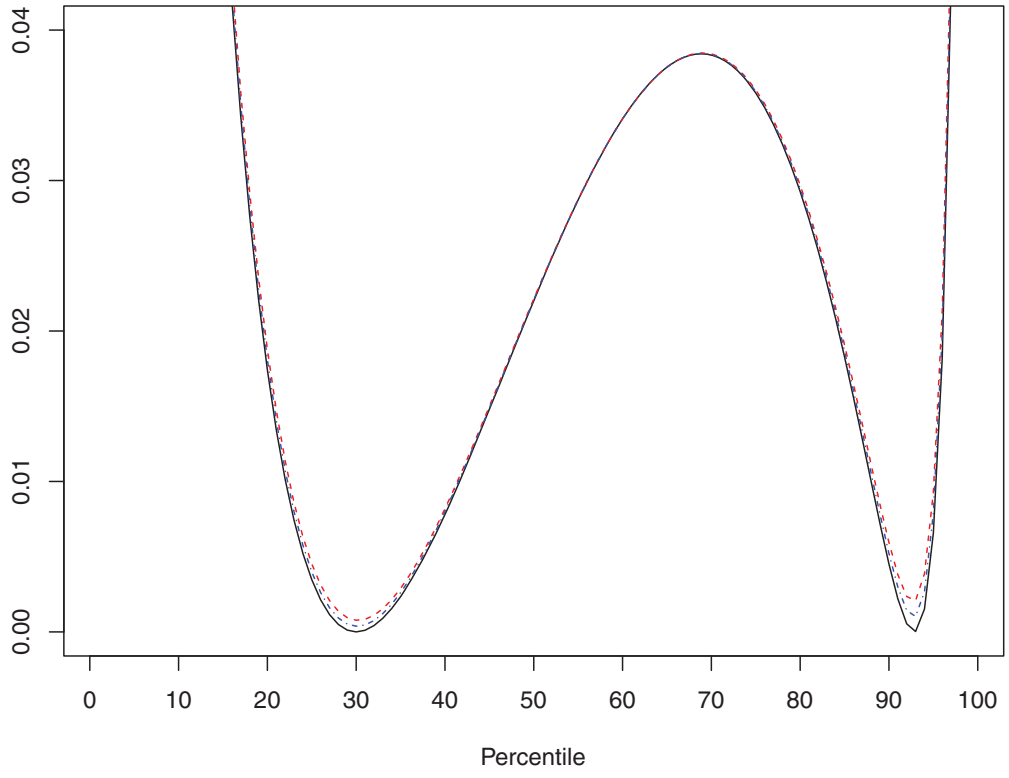

(b)

Fig. 4. Simulation results for ABias and AMSE (a) when an inverse Gaussian distribution was fitted to the Weibull data and (b) when a Weibull distribution was fitted to the inverse Gaussian data (— ABias, $\cdots$ AMSE for $n = 10$, $- \cdot -$ AMSE for $n = 20$).

Table 10. Asymptotic biases and their asymptotic variances when the inverse Gaussian distribution (M_2) was fitted to true Weibull data ($\lambda = 0.1, \beta = 5.0$) and when the Weibull distribution (M_1) was fitted to a true inverse Gaussian distribution ($\mu = 5.0, \kappa = 100.0$)

				AVAR(Bias)				
p	*True distribution*	y_p	*ABias*	$n = 10$	*20*	*50*	*100*	*200*
Quantile								
0.05	M_1	5.5209	0.2877	0.1120	0.0269	0.0044	0.0011	0.0003
	M_2	3.3934	−0.5609	0.0029	0.0014	0.0006	0.0003	0.0001
0.10	M_1	6.3758	−0.0037	0.0900	0.0216	0.0035	0.0009	0.0002
	M_2	3.6741	−0.3548	0.0023	0.0011	0.0004	0.0002	0.0001
0.50	M_1	9.2932	−0.4160	0.0051	0.0012	0.0002	*	*
	M_2	4.8784	0.1484	0.0001	0.0001	*	*	*
0.95	M_1	12.4538	1.1139	0.3323	0.0798	0.0131	0.0032	0.0008
	M_2	7.0210	−0.0810	0.0027	0.0013	0.0005	0.0003	0.0001
MTTF	M_1	9.1817	*	*	*	*	*	*
	M_2	5.0000	−0.0243	0.0031	0.0031	0.0031	0.0031	0.0031

*Indicates that the absolute value is less than 0.0001.

From Equations (18) and (19), it is clear that the PCS is sensitive to the parameter β under the Weibull distribution. For a fixed $\lambda = 0.1$, we performed a sensitivity analysis of PCS against β. We observe from Table 8 that the PCS is negligibly affected by the parameter β and only affected by the sample size n. We also performed sensitivity analysis of the PCS against λ with respect to a fixed β, and observed that the PCS was not affected by the parameter λ either (results not shown). To investigate the effect of these parameters on the PCS under the inverse Gaussian distribution, we performed sensitivity analysis of the PCS for various values of μ and κ. We observe from Table 9 that the parameter κ has little effect on the PCS, but we also observe that the PCS increases as the parameter μ increases. The observations are based on both MC simulation results with 10 000 replications and the large-sample properties of the MLEs under model mis-specification between the Weibull and inverse Gaussian distributions.

To investigate the effect of model mis-specification on the accuracy and precision of quantiles and MTTF, we performed MC simulations with 10 000 replications. The inverse Gaussian distribution was fitted to the Weibull data with parameters $\lambda = 0.1$ and $\beta = 5.0$. The ABias for MTTF was zero as expected (Table 10) and its AVARs were almost zero regardless of the sample size, which means that the effect of model mis-specification on the accuracy and precision of the product's MTTF is negligible even for moderate sample sizes. Figure 4(a) shows that the Abiases and AMSEs are at a minimum at $p = 0.10$ and $p = 0.80$ and at a maximum around $p = 0.4$. It is interesting to note that the AVARs are almost zero around the median. Next, the Weibull distribution was fitted to true inverse Gaussian data with parameters $\mu = 5.0$ and $\kappa = 100.0$. The ABiases for p on two tails are negative (Table 10), which means that the estimated quantiles would be overestimated if the inverse Gaussian distribution was treated as a Weibull distribution. We also observe (see Fig 4(b)), that the Abiases and the AMSEs are at a minimum at $p = 0.30$ and $p = 0.93$ and at a maximum around $p = 0.7$. In both scenarios, the ABiases for quantiles and MTTF are constant regardless of the sample size, because these asymptotic biases depend only on the model parameters.

6. Concluding remarks

Motivated by the shock test data of SMP display modules, we investigated how to discriminate between the Weibull and inverse Gaussian distributions and discussed the effects of model mis-specification. These two distributions assume weakest link failure and cumulative shock failure, respectively. We used the MLE method to estimate the parameters of the two distributions and obtained the asymptotic distributions of the ratio of the MLE functions. Using the asymptotic results, we then computed the PCS to select the best model and then used the PCS to derive the minimum sample size required to discriminate between Weibull and inverse Gaussian distributions for a user-specified protection level. The analytical results showed that shock test data for SMP display modules was better fitted by the inverse Gaussian distribution than the Weibull distribution, lending support to a cumulative shock failure mechanism. We also addressed the effect of model mis-specification based on the product's quantiles and MTTF analytically using MC simulations. The simulation results revealed that mis-specification of the underlying distribution (Weibull for inverse Gaussian or *vice versa*) had a negligible effect on the accuracy and precision of the product's MTTF, even for moderate sample sizes.

In future research, the formulas given here can be used to study the coverage of true values of Weibull and inverse Gaussian large-sample confidence intervals when there is

model mis-specification. This would be of great interest to a practitioner interested in the range of values thought to contain the quantile or probability of interest, rather than point estimates. Furthermore, we did not cover censored data in this study, but the ability to discriminate between Weibull and inverse Gaussian distributions for censored data is worthy of future research.

Acknowledgements

The authors are grateful to the referees for their careful reading and helpful suggestions. The authors thank Professor Sheng-Tsaing Tseng for helpful comments when he visited National Center for Theoretical Sciences at National Tsing Hua University, Taiwan.

Funding

This work was supported by Mid-career Researcher Program through National Research Foundation of Korea (NRF) grant funded by the MEST (2011-0016598).

References

ASTM. (1999) ASTM D332-99. *Standard Test Methods for Mechanical-Shock Fragility of Products Using Shock Machines*.

Atkinson, A. (1970) A method for discriminating between models (with discussions). *Journal of the Royal Statistical Society B*, **40**, 323–353.

Bain, L.J. and Englehardt, M. (1980) Probability of correct selection of Weibull versus gamma based on livelihood ratio. *Communications in Statistics - Theory and Methods*, **9**, 375–381.

Chambers, E.A. and Cox, D.R. (1967) Discriminating between alternative binary response models. *Biometrika*, **54**, 573–578.

Chen, W.W. (1980) On the tests of separate families of hypotheses with small sample size. *Journal of Statistical Computations and Simulations*, **2**, 183–187.

Chhikara, R.S. and Folks, J.L. (1989) *The Inverse Gaussian Distribution: Theory, Methodology, and Applications*, Marcel Dekker, New York, NY.

Cox, D.R. (1961) Tests of separate families of hypothesis, in *Proceedings of the Fourth Berkeley Symposium in Mathematical Statistics and Probability*, University of California Press, Berkeley, CA, pp. 105–123.

Dumonceaux, R. and Antle, C.E. (1973) Discriminating between the log-normal and Weibull distribution. *Technometrics*, **15**, 923–926.

Durham, S.D. and Padgett, W.J. (1997) Cumulative damage models for system failure with application to carbon fibers and composites. *Technometrics*, **39**, 34–44.

Fearn, D.H. and Nebenzahl, E. (1991) On the maximum likelihood ratio method of deciding between the Weibull and gamma distributions. *Communications in Statistics - Theory and Methods*, **20**, 579–593.

Goyal, S., Papadopoulos, J.M. and Sullivan, P.A.(1997) Shock protection of portable electronic products: shock response spectrum, damage boundary approach, and beyond. *Shock and Vibration*, **4**, 169–171.

Gupta, R.D. and Kundu, D. (1951) Discriminating between Weibull and generalized exponential distributions. *Computational Statistics & Data Analysis*, **43**, 179–196.

Kullback, S. and Leibler, R.A. (1951) On information and sufficiency. *Annals of Mathematical Statistics*, **22**, 79–86.

Kundu, D., Gupta, R.D. and Manglick, A. (2005) Discriminating between the log-normal and generalized exponential distributions. *Journal of Statistical Planning and Inference*, **127**, 213–227.

Kundu, D. and Manglick, A. (2004) Discriminating between the Weibull and log-normal distributions. *Naval Research Logistics*, **51**, 893–905.

Kundu, D. and Manglick, A. (2005) Discriminating between the log-normal and gamma distributions. *Journal of the Applied Statistical Sciences*, **14**, 175–187.

Lim, C.-T., Teo, Y.M. and Shim, V.P.W. (2002) Numerical simulation of the drop impact response of a portable electronic product. *IEEE Transactions on Components and Packaging Technologies*, **25**(3), 478–485.

Meeker, W.Q. and Escobar, L.A. (1998) *Statistical Methods for Reliability Data*, Wiley, New York, NY.

Newton, R.E. (1968) *Fragility Assessment Theory and Test Procedure*, Monterey Research Laboratory, Inc., Monterey, CA.

Onar, A. and Padgett, W.J. (2000) Inverse Gaussian accelerated test models based on cumulative damage. *Journal of Statistical Computation and Simulation*, **64**, 233–247.

Pascual, F.G. (2005) Maximum likelihood estimation under misspecified log-normal and Weibull distributions. *Communications in Statistics-Simulation and Computations*, **34**, 503–524.

Pereira, B.B. (1978) Empirical comparisons of some tests of separate families of hypotheses. *Metrika*, **25**, 219–234.

Quesenberry, C.P. and Kent, J. (1982) Selecting among probability distributions used in reliability. *Technometrics*, **24**, 59–65.

Tsai, C.-C., Tseng, S.-T. and Balakrishnan, N. (2011) Mis-specification analyses of gamma and Wiener degradation processes. *Journal of Statistical Planning and Inference*, **141**, 3725–3735.

White, H. (1982a) Maximum likelihood estimation of misspecified models. *Econometrica*, **50**, 1–25.

White, H. (1982b) Regularity conditions for Cox's test of non-nested hypotheses. *Journal of Econometrics*, **19**, 301–318.

Yu, H.-F. (2007) Mis-specification analysis between normal and extreme value distributions for a linear regression model. *Communications in Statistics-Theory and Methods*, **36**, 499–521.

Appendices

Appendix A: Expressions for $\mathbf{A}(\theta_i : \theta_j)$ and $\mathbf{B}(\theta_i : \theta_j)$

In this section, we provide the formulas used to compute the AVCV matrix of QMLEs when there is model mis-specification. The elements in $\mathbf{A}(\theta_1 : \theta_2)$ with respect to M_1 can be expressed as follows:

$$E_{M_1}\left(\frac{\partial^2 \mathcal{L}(\theta_2)}{\partial \mu^2}\right) = \frac{2n\kappa}{\mu^3} - \frac{3n\kappa}{\mu^4 \lambda\beta}\Gamma\left(\frac{1}{\beta}\right),$$

$$E_{M_1}\left(\frac{\partial^2 \mathcal{L}(\theta_2)}{\partial \mu \partial \kappa}\right) = \frac{n}{\mu^3 \lambda\beta}\Gamma\left(\frac{1}{\beta}\right) - \frac{n}{\mu^2},$$

$$E_{M_1}\left(\frac{\partial^2 \mathcal{L}(\theta_2)}{\partial \kappa^2}\right) = -\frac{n}{2\kappa^2}.$$

The elements in $\mathbf{B}(\Theta_1 : \Theta_2)$ can be expressed as follows:

$$E_{M_1}\left(\frac{\partial\mathcal{L}(\Theta_2)}{\partial\mu}\frac{\partial\mathcal{L}(\Theta_2)}{\partial\mu}\right) = E_{M_1}\left[\left(\frac{\kappa}{\mu^3}\sum_{i=1}^{n}x_i - \frac{n\kappa}{\mu^2}\right)^2\right],$$

$$E_{M_1}\left(\frac{\partial\mathcal{L}(\Theta_2)}{\partial\mu}\frac{\partial\mathcal{L}(\Theta_2)}{\partial\kappa}\right) = E_{M_1}\left[\left(\frac{\kappa}{\mu^3}\sum_{i=1}^{n}x_i - \frac{n\kappa}{\mu^2}\right)\left(\frac{n}{2\kappa} + \frac{n}{\mu} - \frac{1}{2\mu^2}\sum_{i=1}^{n}x_i - \frac{1}{2}\sum_{i=1}^{n}x_i^{-1}\right)\right],$$

$$E_{M_1}\left(\frac{\partial\mathcal{L}(\Theta_2)}{\partial\kappa}\frac{\partial\mathcal{L}(\Theta_2)}{\partial\kappa}\right) = E_{M_1}\left[\left(\frac{n}{2\kappa} + \frac{n}{\mu} - \frac{1}{2\mu^2}\sum_{i=1}^{n}x_i - \frac{1}{2}\sum_{i=1}^{n}x_i^{-1}\right)^2\right].$$

At this time, the elements in $\mathbf{A}(\Theta_2 : \Theta_1)$ with respect to M_2 have the following form:

$$E_{M_2}\left(\frac{\partial^2\mathcal{L}(\Theta_1)}{\partial\lambda^2}\right) = -\frac{n\beta}{\lambda^2} + \beta(\beta-1)\lambda^{\beta-2}\sum_{i=1}^{n}E_{M_2}\left(x_i^{\beta}\right),$$

$$E_{M_2}\left(\frac{\partial^2\mathcal{L}(\Theta_1)}{\partial\lambda\partial\beta}\right) = \frac{n}{\lambda} + \left(\beta^2+1\right)\lambda^{\beta-1}\sum_{i=1}^{n}E_{M_2}\left(x_i^{\beta}\right),$$

$$E_{M_2}\left(\frac{\partial^2\mathcal{L}(\Theta_1)}{\partial\beta^2}\right) = -\frac{n}{\beta^2} - \lambda^{\beta}\sum_{i=1}^{n}\left\{(\ln\lambda)^2 E_{M_2}\left(x_i^{\beta}\right) + 2\ln\lambda\frac{\partial E_{M_2}\left(x_i^{\beta}\right)}{\partial\beta} + \frac{\partial^2 E_{M_2}\left(x_i^{\beta}\right)}{\partial\beta^2}\right\}.$$

The elements in $\mathbf{B}(\Theta_2 : \Theta_1)$ have the following expressions:

$$E_{M_2}\left(\frac{\partial\mathcal{L}(\Theta_1)}{\partial\lambda}\frac{\partial\mathcal{L}(\Theta_1)}{\partial\lambda}\right) = E_{M_2}\left[\left(\frac{n\beta}{\lambda} + \beta\lambda^{\beta-1}\sum_{i=1}^{n}x_i^{\beta}\right)^2\right],$$

$$E_{M_2}\left(\frac{\partial\mathcal{L}(\Theta_1)}{\partial\lambda}\frac{\partial\mathcal{L}(\Theta_1)}{\partial\beta}\right) = E_{M_2}\left[\left(\frac{n\beta}{\lambda} + \beta\lambda^{\beta-1}\sum_{i=1}^{n}x_i^{\beta}\right)\times\left(\frac{n}{\beta} + n\ln\lambda + \sum_{i=1}^{n}\left\{\ln x_i - \beta\lambda^{\beta}x_i^{\beta-1}\right\}\right)\right],$$

$$E_{M_2}\left(\frac{\partial\mathcal{L}(\Theta_1)}{\partial\beta}\frac{\partial\mathcal{L}(\Theta_1)}{\partial\beta}\right) = E_{M_2}\left[\left(\frac{n}{\beta} + n\ln\lambda + \sum_{i=1}^{n}\left\{\ln x_i - \beta\lambda^{\beta}x_i^{\beta-1}\right\}\right)^2\right].$$

Appendix B: Approximation of $E_{M_1}(Q)$

By plugging (μ^*, κ^*) into Equation (18), for $\ln\kappa^* = -\ln\lambda_0 - \ln\Upsilon(\beta_0)$, and $\kappa^*/\mu^* = \beta_0\Gamma(1/\beta_0)^{-1}\Upsilon(\beta_0)^{-1}$:

$$\begin{aligned}\frac{E_{M_1}\left(\mathcal{L}_{\mathrm{IG}}(\mu^*,\kappa^*)\right)}{n} &= E_{M_1}\left(\frac{1}{2}\ln\kappa^* - \frac{1}{2}\ln(2\pi) - \frac{3}{2}\ln x - \frac{1}{2}\frac{\kappa^*}{\mu^{*2}}x + \frac{\kappa^*}{\mu^*} - \frac{\kappa^*}{2}x^{-1}\right)\\ &= -\frac{1}{2}\ln\lambda_0 - \frac{1}{2}\ln\Upsilon(\beta_0) - \frac{1}{2}\ln(2\pi) + \frac{3}{2}\left(\ln\lambda_0 + \frac{\gamma}{\beta_0}\right) + \frac{\beta_0}{2}\Gamma\left(\frac{1}{\beta_0}\right)^{-1}\Upsilon(\beta_0)^{-1} - \frac{1}{2}\Gamma\left(1-\frac{1}{\beta_0}\right)\Upsilon(\beta_0)^{-1},\end{aligned}$$

where $(\beta_0/2)\Gamma(1/\beta_0)^{-1}\Upsilon(\beta_0)^{-1} - (1/2)\Gamma(1-1/\beta_0)\Upsilon(\beta_0)^{-1} = -1/2$, and

$$\begin{aligned}\frac{E_{M_1}(\mathcal{L}_{\mathrm{WE}}(\lambda_0,\beta_0))}{n} &= E_{M_1}\left(\ln\beta_0 + \beta_0\ln\lambda_0 + (\beta_0-1)\ln x - \lambda_0^{\beta_0}x^{\beta_0}\right)\\ &= \ln\beta_0 + \beta_0\ln\lambda_0 - (\beta_0-1)\left(\ln\lambda_0 + \frac{\gamma}{\beta_0}\right) - 1,\end{aligned}$$

because $E_{M_1}\left((\lambda x)^{\beta}\right) = 1$. Accordingly,

$$\begin{aligned}&\frac{E_{M_1}\left(\mathcal{L}_{\mathrm{IG}}(\mu^*,\kappa^*)\right)}{n} - \frac{E_{M_1}(\mathcal{L}_{\mathrm{WE}}(\lambda_0,\beta_0))}{n}\\ &= -\frac{1}{2}\ln\Upsilon(\beta_0) + \frac{1}{2}(1-\ln(2\pi)) + \frac{\gamma}{2}\left(2+\frac{1}{\beta_0}\right) - \ln\beta_0.\end{aligned}$$

Biographies

Minsu Kim is a Senior Engineer in the Team of Development at Samsung Display Co., Cheonan, Korea. He received his master's degree in the Department of Industrial Engineering at Hanyang University, Seoul, Korea. He has research interest in reliability evaluation for mobile devices, design of experiments, computer-aided experiments, and shock analysis.

Suk Joo Bae is an Associate Professor in the Department of Industrial Engineering at Hanyang University, Seoul, Korea. He received his Ph.D. from the School of Industrial and Systems Engineering at the Georgia Institute of Technology in 2003. He worked as a reliability engineer at Samsung SDI, Korea, from 1996 to 1999. His research interests are centered on reliability evaluation of light displays and nano-devices via accelerated life and degradation testing, statistical robust parameter design, and process control for large-volume online processing data. He has published about 30 papers in journals such as *Technometrics*, *Journal of Quality Technology*, *IIE Transactions*, *IEEE Transactions on Reliability*, and *Reliability Engineering & System Safety*. He is currently an Associate Editor for *IEEE Transactions on Reliability*. He is a member of INFORMS and ASA.